

Eucalyptus scab and shoot malformation: A new and serious foliar disease of *Eucalyptus* caused by *Elsinoe necatrix* sp. nov

Nam Q. Pham¹  | Seonju Marincowitz²  | Myriam Solís²  | Tuan A. Duong²  |
Brenda D. Wingfield²  | Irene Barnes²  | Bernard Slippers²  | Jupiter I. Muro Abad³  |
Alvaro Durán⁴  | Michael J. Wingfield¹ 

¹Department of Plant and Soil Sciences, Forestry and Agricultural Biotechnology Institute (FABI), University of Pretoria, Pretoria, South Africa

²Department of Biochemistry, Genetics and Microbiology, Forestry and Agricultural Biotechnology Institute (FABI), University of Pretoria, Pretoria, South Africa

³Research and Development, PT. Toba Pulp Lestari (TPL), Porsea, North Sumatra, Indonesia

⁴Plant Health Program, Research and Development, Asia Pacific Resources International Holdings Ltd. (APRIL), Pangkalan Kerinci, Riau, Indonesia

Correspondence

Michael J. Wingfield, Department of Plant and Soil Sciences, Forestry and Agricultural Biotechnology Institute (FABI), University of Pretoria, Pretoria 0028, South Africa.
Email: mike.wingfield@fabi.up.ac.za

Abstract

In 2014, a new and serious leaf and shoot disease of unknown aetiology appeared in *Eucalyptus* plantations of North Sumatra, Indonesia. The disease is characterized by black necrotic spots that initially appear on young leaves and petioles, which become scab-like as the lesions age. Infected trees respond to infection by producing shoots with small leaves that commonly appear feathered. Fruiting structures typical of most foliar pathogens are not seen, but using scanning electron microscopy (SEM), fungal spores are evident and associated with the scab-like structures. Using culture-dependent methods, cultures resembling a species of *Elsinoe* were isolated from the lesions. DNA sequence comparisons for four gene regions, as well as morphological observations, showed that the fungus is an undescribed species in *Elsinoe*, for which the name *Elsinoe necatrix* sp. nov. is provided. Pathogenicity trials on a *Eucalyptus* clone with the *Elsinoe* species resulted in scab-like structures similar to those observed under field conditions and the fungus was easily reisolated from the resulting lesions. This study includes a description of the pathogen and characterization of the disease, for which the name Eucalyptus scab and shoot malformation is suggested.

KEYWORDS

fungal pathogens, plantation forestry, scab disease, tree disease

1 | INTRODUCTION

Planted forests in the tropics and the Southern Hemisphere are currently dominated by nonnative plants, especially species of *Eucalyptus* (Payn et al., 2015). They are generally short-rotation plantations, usually of clones representing highly productive interspecific hybrids (Cossalter & Pye-Smith, 2003). These plantations offer great benefits, but this practice also raises challenges regarding the susceptibility of individual clones to pests and diseases (Old et al., 2003; Paine et al., 2011).

During the early establishment of *Eucalyptus* plantations in new habitats, trees are often not seriously affected by diseases or pest problems (Hurley et al., 2016; Wingfield et al., 2015). This is partly

due to their separation from the pathogens and insects that affect them under natural conditions (Wingfield et al., 2008, 2010). However, this situation changes over time where these emerging diseases of planted forests can be due either to exotic pathogens accidentally introduced into *Eucalyptus* plantation areas, typically through anthropogenic activities, or alternatively to endemic organisms that have adapted to infect new hosts (Burgess & Wingfield, 2017; Ghelardini et al., 2016; Wingfield et al., 2010).

For *Eucalyptus* plantation forestry, other than some well-known diseases including vascular wilt, stem canker, and root rot, foliar and shoot diseases are of particular concern (Keane et al., 2000). Amongst the most important pathogens are the rust fungus *Austropuccinia psidii* (Carnegie et al., 2016; Coutinho et al., 1998;

Glen et al., 2007), *Calonectria* spp. (Alfenas et al., 2015; Crous, 2002; Lombard et al., 2015; Pham et al., 2019), and a few species belonging to the Mycosphaerellaceae and Teratosphaeriaceae (Andjic et al., 2019; Greyling et al., 2016; Hunter et al., 2011; Old et al., 2003; Wingfield et al., 1996).

In 2014, a new *Eucalyptus* shoot and foliar disease of unknown aetiology appeared in the plantations in the Lake Toba area of North Sumatra. The disease is widespread in the affected area, covering approximately 40,000 ha on *Eucalyptus* in the subgenus *Symphyomyrtus* and hybrids of these species. The disease symptoms were closely linked to periods of rainfall and were characterized by malformation of the growing shoots. Fruiting bodies, typical of known *Eucalyptus* pathogens, were not present and the symptoms were unlike any other foliar or shoot diseases known in *Eucalyptus*

plantations elsewhere in the world. The disease has continued to damage plantations in the affected area since its first appearance. The aim of this study was to identify the causal agent of the disease based on isolations from affected *Eucalyptus* tissues, multigene phylogenetic analyses of resulting cultures, and pathogenicity tests.

2 | MATERIALS AND METHODS

2.1 | Disease prevalence and symptoms

Disease symptoms (Figure 1) appear shortly after the onset of rain and trees begin to recover at the onset of dry periods. The disease is most obvious on young trees in the first year or two of growth. The



FIGURE 1 Symptoms on *Eucalyptus* associated with *Eucalyptus* scab and shoot malformation. (a) Black necrotic spots surrounded by a yellow halo typical of early symptoms. (b) Slightly raised, diffuse margins of the infections becoming scab-like as they age. (c) Concentrated scabs where rainwater accumulates on the leaf surface. (d) Scabs leading to deformation of a leaf, causing curvature, usually on one of the leaf lobes. (e) Girdled, crinkled, and distorted shoots and leaves. (f) "Feathering" effect at the apices of trees, a typical secondary symptom on some clones

first obvious symptoms are elongated growing shoots and small deformed leaves. These symptoms differ depending on the *Eucalyptus* clones planted, which mostly include hybrids of *Eucalyptus grandis* and *Eucalyptus urophylla* (*Eu. grandis* × *Eu. urophylla*), and that differ distinctly in their relative susceptibility.

Young leaf and shoot tissues are most severely affected. Small necrotic spots that are up to 1 mm in diameter appear on these tissues, which are circular or irregular, brown to black in colour and sometimes surrounded by a yellow chlorotic halo (Figure 1a). As infection develops, the spots become reddish brown to black at their centres with slightly raised, diffuse, tan to grey, scabby margins (Figure 1b–d). Spots can be scattered (Figure 1a) or concentrated where rainwater accumulates on the leaf surface (Figure 1c). This eventually leads to deformation of the leaves, causing curvature usually on one of the leaf lobes (Figure 1d). The scab-like spots commonly dry and drop, causing a shot-hole appearance.

In severely affected trees, lesions can coalesce, leading to girdled, crinkled, and distorted shoots and leaves (Figure 1e). Once the leaves are infected, the damage to the tissues is permanent, and the infected tissues do not recover. In more susceptible clones, secondary symptoms include a “feathering” effect, resulting in loss of apical dominance, abnormal elongated branches with short internodes, and the production of epicormic shoots (Figure 1f). Severely affected clones usually die after a number of successive infection cycles, generally over a period of 2–3 years.

2.2 | Isolations from tissues with symptoms

Isolations were made from necrotic leaf spots that developed during the infection cycles in January and November 2018 and January 2020. The sampling sites were selected to cover the elevation and geographic range of infected *Eucalyptus* plantations. At each site, approximately 20 plants were randomly selected for sample collection. Freshly infected young leaves and shoots were collected, stored in paper bags, and transported to the laboratory for isolation. The infected leaves were surface disinfested by spraying with 70% ethanol, washed with distilled water, dried with sterile paper towels, and infections located using a dissection microscope. Leaf spots were carefully lifted from the leaf surface using a sterile needle and placed on the surface of malt extract agar (MEA; 20 g malt extract, 20 g Difco agar, 1 L ionized water) amended with 100 µg chloramphenicol (Sigma-Aldrich) and 1 ml lactic acid. Isolation plates were incubated for 5–7 days at 25 °C until colonies began to grow from the tissues with symptoms.

Pure cultures were established by transferring hyphal tips to fresh MEA. All the isolates generated in this study were deposited in the culture collection (CMW) of the Forestry and Agricultural Biotechnology Institute (FABI), University of Pretoria, South Africa. Representative isolates, including an ex-type culture, were deposited in the culture collection (CBS) of the Westerdijk Fungal Biodiversity Institute, Utrecht, Netherlands. The dried type specimen was deposited in the National Collection of Fungi (PREM), Roodeplaat, Pretoria, South Africa.

2.3 | DNA extraction, PCR amplification, and sequencing

Isolates of the putative pathogen were subjected to identification based on DNA sequence analyses. DNA was extracted from the 3-week-old isolates grown on 2% MEA at 25 °C, using Prepman Ultra Sample Preparation Reagent (Thermo Fisher Scientific) following the manufacturer's protocols. The internal transcribed spacer regions 1 and 2 (ITS), including the 5.8S rRNA region, were amplified using primers ITS1 and ITS4 (White et al., 1990); the nuclear large subunit (LSU) of ribosomal RNA with primers LROR and LR5 (Rehner & Samuels, 1994; Vilgalys & Hester, 1990); part of the DNA-directed RNA polymerase II second largest subunit (*RPB2*) with primer pair *RPB2-5F2* and *rRBP2-7cR* (Liu et al., 1999; Sung et al., 2007); and a fragment of the translation elongation factor 1- α (*TEF1*) using primers *elongation-1-F* and *elongation-1-R* (Hyun et al., 2007).

PCR amplifications were prepared following the protocols described by Pham et al. (2019) and conditions for PCR were as recommended by Fan et al. (2017). ExoSAP-IT PCR Product Cleanup Reagent (Thermo Fisher Scientific) was used to purify amplified fragments. PCR products were sequenced in both directions using the same primers used for amplification with the BigDye terminator sequencing kit v. 3.1 (Applied Biosystems). Sequences were obtained on an ABI PRISM 3100 DNA sequencer (Applied Biosystems) at the Sequencing Facility of the Faculty of Natural and Agricultural Sciences, University of Pretoria, Pretoria, South Africa. Raw sequence reads were assembled and edited using Geneious v. 7.0 (Kearse et al., 2012).

2.4 | Phylogenetic analyses

Preliminary identification was made by performing a nucleotide BLAST search using the ITS region sequences against the NCBI GenBank database (<http://www.ncbi.nlm.nih.gov/>) to identify the isolates to genus and closest species level. Sequences for the isolates of the putative pathogen were compared with data for previously published species downloaded from GenBank to generate the data sets for further phylogenetic analyses. All sequences were aligned using MAFFT v. 7 (<http://mafft.cbrc.jp/alignment/server/>) (Kato and Standley, 2013), then confirmed visually in MEGA v. 7 where necessary. Sequences for the isolates of the putative pathogen were deposited in GenBank.

Phylogenetic analyses including maximum likelihood (ML) and Bayesian inference (BI) were conducted for the single gene sequence data sets of the ITS, LSU, *RPB2*, and *TEF1*, and the combined data set of all four gene regions. The most appropriate model was obtained using the software jModeltest v. 1.2.5. (Posada, 2008). ML analyses were conducted using RaxML v. 8.2.4 on the CIPRES Science Gateway v. 3.3 (Stamatakis, 2014) with default GTR substitution matrix and 1,000 rapid bootstraps. BI analyses were conducted using MrBayes v. 3.2.6 (Ronquist et al., 2012) on the CIPRES Science Gateway v. 3.3. Four Markov chain Monte Carlo (MCMC) chains were run from a random starting tree for five million generations

and trees were sampled every 100th generation. The first 25% of trees sampled were discarded as burn-in and the remaining trees were used to calculate the posterior probabilities. *Myriangium hispanicum* (CBS 347.33) was used as the outgroup taxon in all phylogenetic analyses. Final consensus trees were viewed using MEGA v. 7 (Kumar et al., 2016).

2.5 | Microscopy and culture characteristics

Leaves with symptoms and spots were studied using a Nikon Eclipse Ni SMZ18 microscope and Nikon DS-Ri2 camera. In order to study the distribution of the causal fungus within the leaf tissues, sections of leaves including the spots typical of infection were prepared using a CM1520 cryostat (Leica). The sections were 10–12 µm thick and were mounted in 85% lactic acid for observation.

For scanning electron microscopy (SEM), leaf pieces (3 × 3 mm) including the necrotic spots were fixed in 2.5% glutaraldehyde/formaldehyde solution for a minimum of 1 hr. The samples were then washed three times with phosphate buffer for 15 min each. They were dehydrated using an ethanol series (30%, 50%, 70%, 90%) for 15 min each followed by three dehydration steps in 100% ethanol, two for 15 min each and one for 30 min. The dehydrant hexamethyl disilazane (HMDS) was used to perform the critical dehydration of the samples. The dehydrated samples were mounted on aluminium plates and coated with carbon using a Q150T Coating Unit (Quorum). The samples were observed using a 540 Gemini Ultra Plus FEG SEM (Zeiss) at the Laboratory for Microscopy and Microanalysis, University of Pretoria, Pretoria, South Africa.

Culture characteristics and growth rate of the putative causal fungus were determined on potato dextrose agar (PDA; BD Difco). Colony colour was determined using the colour charts of Rayner (1970). A plug of mycelium taken from a 3-week-old culture was placed at the centre of each plate. The cultures were incubated at seven different temperatures ranging from 5 to 35 °C at 5 °C intervals for 30 days in the dark, after which the average diameter was calculated.

2.6 | Pathogenicity tests

To confirm pathogenicity of the putative causal fungus, three isolates (CMW 56129, CMW 56134, and CMW 56137) were selected for inoculation on *Eu. grandis* leaf material under laboratory conditions. The isolates were grown on PDA for 4 weeks at 20 °C. The mycelial inoculum was prepared by first adding sterile distilled water and one drop of Tween 20 (Sigma-Aldrich) to colonies in Petri dishes, after which the colonies were scraped using a sterile spatula and the mycelium filtered through one layer of sterile cheesecloth. The density of the resulting mycelial fragments was measured using a haemocytometer and adjusted to approximately 10⁵ mycelial fragments per ml.

Small branches, 20 cm in length, bearing new shoots and young leaves up to one-quarter of mature size, were harvested from 20-month-old plants. They were inserted into moistened florist foam and sprayed with inoculum until the leaves were uniformly covered. Leaves on five sets of branches were inoculated per isolate, and an equal number of controls were sprayed with sterile distilled water. The branches were placed in square plastic containers that were closed and sealed to retain humidity and ensure the leaf wetness. These were maintained in an isolated growth chamber at 20 °C with artificial day–night cycles and were monitored daily for symptom development.

The inoculated leaves that developed necrotic spots were surface disinfested with 70% ethanol and washed with sterile distilled water. The spots were lifted from the leaf surfaces with a sterilized needle and plated onto MEA amended with 100 µg chloramphenicol. The plates were incubated at 25 °C until the growth of fungal hyphae became visible. To confirm Koch's postulates, resulting isolates were identified based on morphological characteristics and DNA sequences for the ITS region. In addition, lesions resulting from the inoculation tests were observed using SEM where inoculated leaves were harvested and treated as described above.

3 | RESULTS

3.1 | Histopathology of infected tissues

Colonization of fungus within lesions was observed under the microscope (Figure 2). Degraded cuticle and collapsed epidermis cells were seen (Figure 2a). Sterile fungal hyphae were detected in the necrotic lesions, usually above and within collapsed epidermis and parenchyma cells (Figure 2a,e–g). Neighbouring parenchyma cells were thickened, pigmented, often filled with amorphous substance including hyphae (Figure 2b,c). In better developed lesions, extensive host cell division between infected and healthy tissue led to dehiscence of infected cells from the leaves (Figure 2d). However, specialized fungal structures such as conidiophores were not seen under the microscope.

Using SEM, the scab-like lesions appeared to have eroded the host cuticle (Figure 3a,b). Scab-like layers were evident bordering the necrotic areas with slightly raised margins (Figure 3c). Fruiting structures were not seen but fungal spores were associated with the scab-like structures, usually at the centres of the necrotic spots (Figure 3d).

3.2 | Isolations from tissues with symptoms

In total, 14 isolates having a similar morphology and thought to be the causal agent of the *Eucalyptus* disease were obtained from leaf tissues with symptoms (Table 1). Of these, four isolates were collected in 2018 and 10 were from the 2020 sampling. These isolates usually emerged from diseased tissue fragments after 5–7 days and

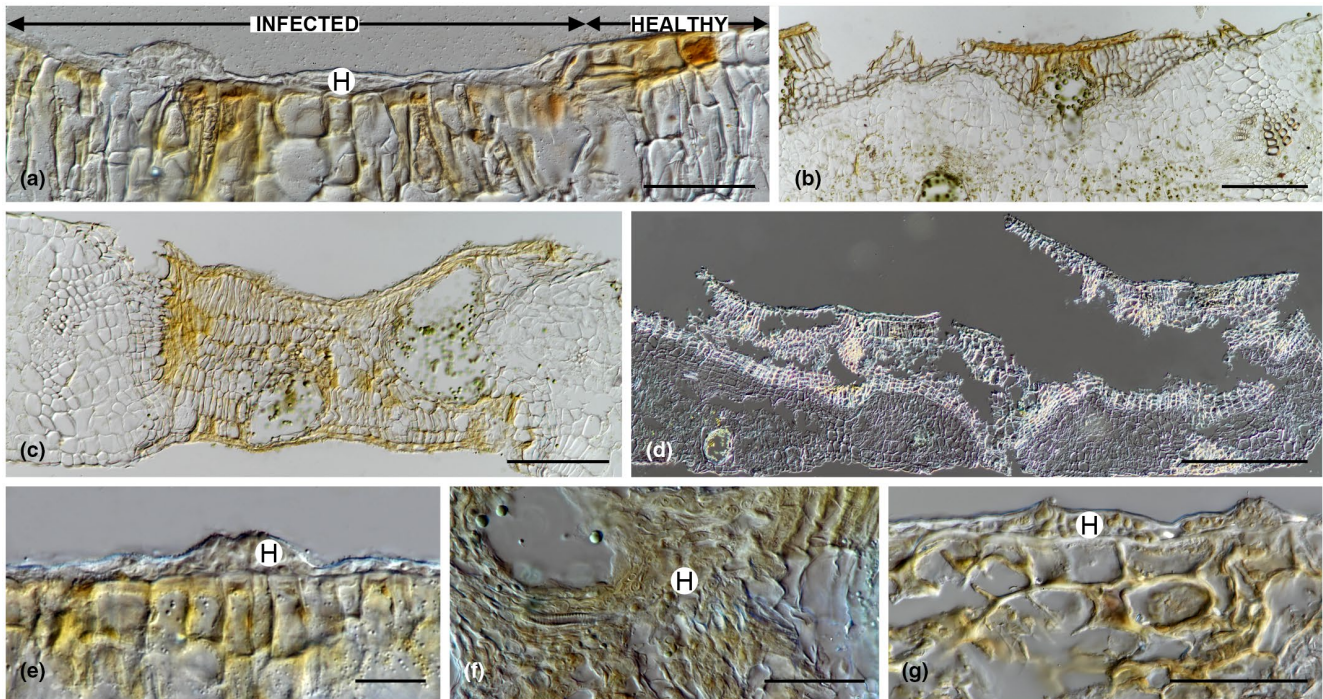


FIGURE 2 Cross-sections through the lesions on the leaves affected by *Eucalyptus* scab and shoot malformation. (a) Section through a lesion showing collapsed cuticle and epidermal cells in contrast to the healthy intact area. (b) Infected region of a leaf showing extensive cell division and thickened cell walls and pigmentation. (c) Necrotic lesion. (d) Dehiscence of scab from leaf. (e–g). Hyphae (H) colonizing above and within epidermis and the parenchyma cells. Scale bars: c = 250 μm ; b, d, f = 100 μm ; a, e, g = 50 μm

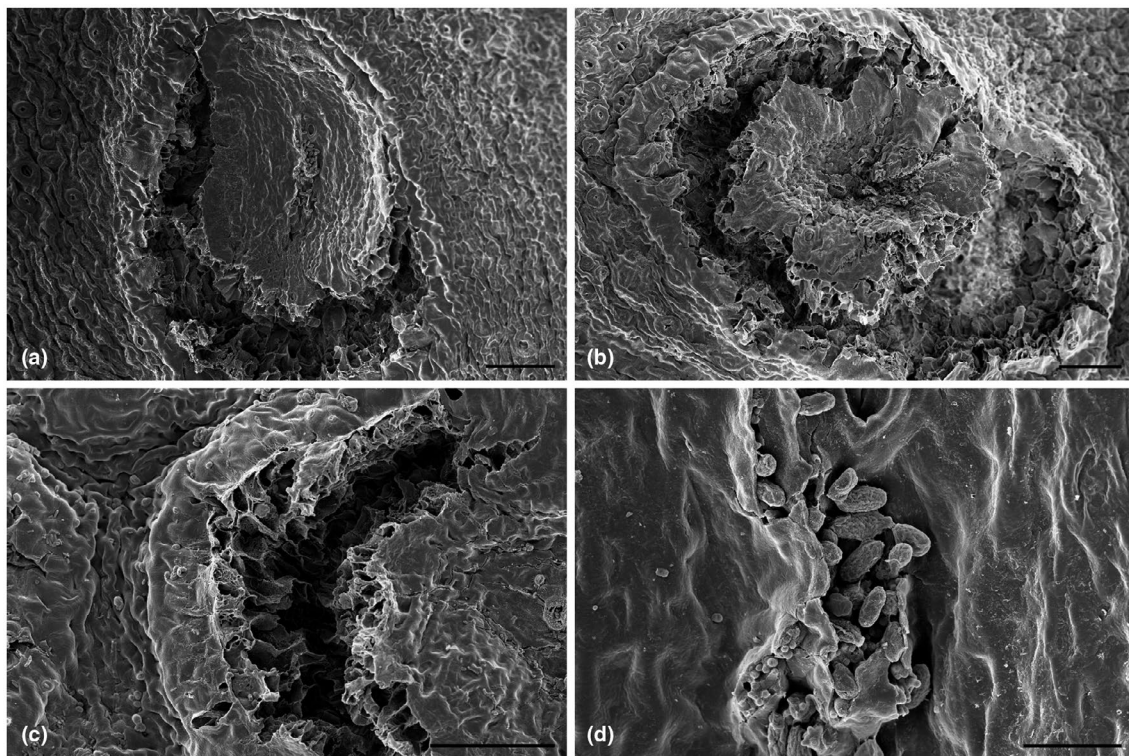


FIGURE 3 Scanning electron micrographs of field-collected leaf tissue with *Eucalyptus* scab and shoot malformation. (a,b) Scab-like necrotic spots with visible erosion of the host cuticle. (c) Scab-like layers bordering the necrotic area with slightly raised margin. (d) Fungal spores observed at the centre of the necrotic area. Scale bars: a–c = 50 μm ; d = 10 μm

TABLE 1 Collection details and GenBank accession numbers of species of *Elsinoe* obtained from this study and other species included in the phylogenetic analyses

Species	Isolates	Host/substrate	Locality	GenBank accession number				References
				ITS	LSU	RPB2	TEF1	
<i>Elsinoe annonae</i>	CBS 228.64	<i>Annona</i> sp.	USA	KX887190	KX886954	KX887073	KX886836	Fan et al. (2017)
<i>Elsinoe caleae</i>	CBS 221.50 ^T	<i>Calea pinnatifida</i>	Brazil	KX887205	KX886968	KX887088	KX886851	Fan et al. (2017)
<i>Elsinoe centrolobii</i>	CBS 222.50 ^T	<i>Centrobium robustum</i>	Brazil	KX887206	KX886969	KX887089	KX886852	Fan et al. (2017)
<i>Elsinoe citricola</i>	CPC 18535 ^T = RWB 1175	<i>Citrus limonia</i>	Brazil	KX887207	KX886970	KX887090	KX886853	Fan et al. (2017)
<i>Elsinoe diospyri</i>	CBS 223.50 ^T	<i>Diospyros kaki</i>	Brazil	KX887210	KX886973	KX887093	KX886856	Fan et al. (2017)
<i>Elsinoe eelemani</i>	DAR 83016 ^T	<i>Melaleuca alternifolia</i>	Australia	KX372292	N/A	KX398204	KX398203	Crous et al. (2016)
<i>Elsinoe erythrinae</i>	CPC 18530 = RWB 1138	<i>Erythrina</i> sp.	Brazil	KX887212	KX886975	KX887094	KX886858	Fan et al. (2017)
<i>Elsinoe eucalypticola</i>	CBS 124765 ^T = CPC 13318	<i>Eucalyptus</i> sp.	Australia	KX887215	KX886978	KX887097	KX886861	Fan et al. (2017)
<i>Elsinoe fagarae</i>	CBS 514.50 ^T	<i>Fagaria riedeliana</i>	Brazil	KX887218	KX886981	KX887100	KX886864	Fan et al. (2017)
<i>Elsinoe fawcettii</i>	CBS 139.25 ^T	<i>Citrus</i> sp.	USA	KX887219	KX886982	KX887101	KX886865	Fan et al. (2017)
<i>Elsinoe fici</i>	CBS 515.50	<i>Ficus luschnathiana</i>	Brazil	KX887223	KX886986	KX887105	KX886869	Fan et al. (2017)
<i>Elsinoe fici-caricae</i>	CBS 473.62 ^T = ATCC 14652	<i>Ficus carica</i>	India	KX887224	KX886987	KX887106	KX886870	Fan et al. (2017)
<i>Elsinoe flacourtae</i>	CBS 474.62 ^T = ATCC 14654	<i>Flacourtia sepriaria</i>	India	KX887225	KX886988	KX887107	KX886871	Fan et al. (2017)
<i>Elsinoe ichnocarpi</i>	CBS 475.62 ^T = ATCC 14655	<i>Ichnocarpus frutescens</i>	India	KX887232	KX886995	KX887114	KX886878	Fan et al. (2017)
<i>Elsinoe jasminae</i>	CBS 224.50 ^T	<i>Jasminum sambac</i>	Brazil	KX887233	KX886996	KX887115	KX886879	Fan et al. (2017)
<i>Elsinoe necatrix</i>	CMW 56126	<i>Eucalyptus</i> sp.	Indonesia	MW079497	MW079515	MW086707	MW086721	This study
	CMW 56127	<i>Eucalyptus</i> sp.	Indonesia	MW079498	MW079516	MW086708	MW086722	This study
	CMW 56128	<i>Eucalyptus</i> sp.	Indonesia	MW079499	MW079517	MW086709	MW086723	This study
	CMW 56129 = CBS 147438	<i>Eucalyptus</i> sp.	Indonesia	MW079500	MW079518	MW086710	MW086724	This study
	CMW 56130	<i>Eucalyptus</i> sp.	Indonesia	MW079501	MW079519	MW086711	MW086725	This study
	CMW 56131	<i>Eucalyptus</i> sp.	Indonesia	MW079502	MW079520	MW086712	MW086726	This study
	CMW 56132	<i>Eucalyptus</i> sp.	Indonesia	MW079503	MW079521	MW086713	MW086727	This study
	CMW 56133	<i>Eucalyptus</i> sp.	Indonesia	MW079504	MW079522	MW086714	MW086728	This study
	CMW 56134 ^T = CBS 147439	<i>Eucalyptus</i> sp.	Indonesia	MW079505	MW079523	MW086715	MW086729	This study
	CMW 56135	<i>Eucalyptus</i> sp.	Indonesia	MW079506	MW079524	MW086716	MW086730	This study
	CMW 56136	<i>Eucalyptus</i> sp.	Indonesia	MW079507	MW079525	MW086717	MW086731	This study
	CMW 56137 = CBS 147440	<i>Eucalyptus</i> sp.	Indonesia	MW079508	MW079526	MW086718	MW086732	This study
	CMW 56138	<i>Eucalyptus</i> sp.	Indonesia	MW079509	MW079527	MW086719	MW086733	This study
	CMW 56139	<i>Eucalyptus</i> sp.	Indonesia	MW079510	MW079528	MW086720	MW086734	This study
<i>Elsinoe pitangae</i>	CBS 227.50 ^T	<i>Eugenia pitanga</i>	Brazil	KX887269	KX887032	KX887150	KX886914	Fan et al. (2017)

(Continues)

TABLE 1 (Continued)

Species	Isolates	Host/substrate	Locality	GenBank accession number					References
				ITS	LSU	RPB2	TEF1		
<i>Elsinoe populi</i>	CBS 289,64	<i>Populus deltoides</i> subsp. <i>deltoides</i>	Argentina	KX887273	KX887036	KX887154	KX886918	Fan et al. (2017)	
<i>Elsinoe preissianae</i>	CBS 142129 ^T	<i>Eucalyptus preissiana</i>	Australia	KY173406	N/A	N/A	N/A	Crous et al. (2016)	
<i>Elsinoe randii</i>	CBS 170.38 ^T	<i>Carya</i> sp.	Brazil	KX887278	KX887041	KX887158	KX886923	Fan et al. (2017)	
<i>Elsinoe tectificae</i>	CBS 124777 ^T = CPC 14594	<i>Eucalyptus tectifera</i>	Australia	KX887292	KX887055	KX887172	KX886937	Fan et al. (2017)	
<i>Elsinoe tiliae</i>	CBS 350.73 = ATCC 24510	<i>Tilia cordata</i>	New Zealand	KX887296	KX887059	KX887176	KX886940	Fan et al. (2017)	
<i>Elsinoe verbenae</i>	CPC 18561 ^T = RWB 1232	<i>Verbena bonariensis</i>	Brazil	KX887298	KX887061	KX887178	KX886942	Fan et al. (2017)	
<i>Elsinoe zizyphi</i>	CBS 378.62 ^T = ATCC 14656	<i>Zizyphus rugosa</i>	India	KX887303	KX887066	KX887183	KX886947	Fan et al. (2017)	
<i>Myriangium hispanicum</i>	CBS 247.33	<i>Acer monspessulanum</i>	N/A	KX887304	KX887067	KX887184	KX886948	Fan et al. (2017)	

Note: N/A represents information that is not available. Isolates obtained in this study are indicated in bold. ^T denotes ex-type strain.

Abbreviations: ATCC, American Type Culture Collection, Virginia, USA; CBS, culture collection of Westerdijk Fungal Biodiversity Institute, Utrecht, Netherlands; CMW, culture collection of the Forestry and Agricultural Biotechnology Institute (FABI), University of Pretoria, Pretoria, South Africa; CPC, culture collection of Pedro Crous, housed at Westerdijk Fungal Biodiversity Institute; DAR, Plant Pathology Herbarium, New South Wales, Australia; RWB, personal collection of Robert Barreto; ITS, internal transcribed spacer regions 1 and 2 including the 5.8S region of ribosomal RNA; LSU, nuclear large subunit (28S) of ribosomal RNA; RPB2, DNA-directed RNA polymerase II second largest subunit gene; TEF1, translation elongation factor 1- α gene.

grew extremely slowly on MEA. All isolates produced dark red to brown, raised, cerebriform colonies, sometimes with white aerial mycelium on their surfaces. The colonies also produced a distinct red to dark red pigment that diffused into the growth medium.

3.3 | Phylogenetic analysis

An initial BLAST search using sequences for the ITS region against the NCBI GenBank database indicated that the cultures were those of an *Elsinoe* species, with the highest similarity to *Elsinoe ichnocarpi* (94% identity to NR_148147) and *Elsinoe eucalypticola* (94% to NR_132834). The four gene regions were successfully amplified for all 14 cultures, resulting in DNA sequence data of approximately 550, 820, 840, and 390 bp for the ITS, LSU, RPB2, and TEF1 regions, respectively.

For the phylogenetic analyses of each individual data set, the TIM2+I+G model was selected for ITS, TrN+I+G model for LSU and RPB2, and the TrN+G for TEF1. The ML tree for each individual gene region with bootstrap support values of ML and posterior probabilities of BI are presented in Figure S1.

The combined sequence data set used in the phylogenetic analyses included 37 ingroup taxa. Concatenated sequence alignments of the four gene regions together with closely related *Elsinoe* species were deposited in TreeBASE (27059). The TIM2+I+G model was selected for the combined data set. ML and BI analyses resulted in phylogenetic trees with concordant topologies and showed similar phylogenetic relationships between taxa. The ML tree with bootstrap support values of the ML and the posterior probabilities obtained from BI is presented in Figure 4. All the isolates considered in this study clustered in a well-supported clade (ML/BI = 100/1.00), clearly distinct from the most closely related species, that is, *El. eucalypticola* (CBS 124765) and *Elsinoe eelemani* (DAR 83016).

3.4 | Taxonomy

Based on the multigene phylogenetic analyses, the 14 isolates of the *Elsinoe* species from *Eucalyptus* tissues with symptoms represented an undescribed species. This species is characterized as follows:

***Elsinoe necatrix* N.Q. Pham, Marinc. & M.J. Wingf., sp. nov.**

(Figure 5)

Mycobank MB838388

Etymology: "necatrix" (Latin) = killer, murderess, referring to the destructive impact that the disease has on its *Eucalyptus* hosts.

Colonies on PDA in dark for 30 days sterile, raised, irregular shape with lobate edge, convoluted, densely compact causing cracks on medium, covered with short, white, yellow to brown, aerial hairs giving velvety texture over entire cerebriform colony, watery droplets commonly seen on old colonies, above umber to brown vinaceous (7^{mm}) with patches of different shades of hazel (17^{mm}), reverse fuscous black (7^{mm}), under UV light dark above

ITS+LSU+RPB2+TEF1



FIGURE 4 Phylogenetic tree based on maximum likelihood (ML) analysis of a combined DNA data set of ITS, LSU, RPB2, and TEF1 sequences for *Elsinoe* spp. Bootstrap values $\geq 60\%$ for ML analyses and posterior probabilities values ≥ 0.9 obtained from Bayesian inference (BI) are indicated at the nodes as ML/BI. Bootstrap values $< 60\%$ or probabilities values < 0.9 are marked with "*", and nodes lacking the support values are marked with "-". Isolates representing ex-type material are marked with "T". *Myriangium hispanicum* (isolate CBS 247.33) represents the outgroup

chestnut (7' m), reverse fuscous black (7''''''k); some ball-like structures formed on old colonies, consisting of pseudoparenchymatous cells, sterile.

Optimal growth temperature at 25 °C, no growth at 5 and 35 °C; after 30 days, colonies at 10 °C reaching 10.0 mm, at 15 °C 13.0 mm, at 20 °C 16.7 mm, at 25 °C 22.3 mm, and at 30 °C 15.2 mm.

Specimens examined: INDONESIA, North Sumatra, leaf of *Eucalyptus* sp. with symptoms, Mar 2020, N.Q. Pham, PREM 63209,

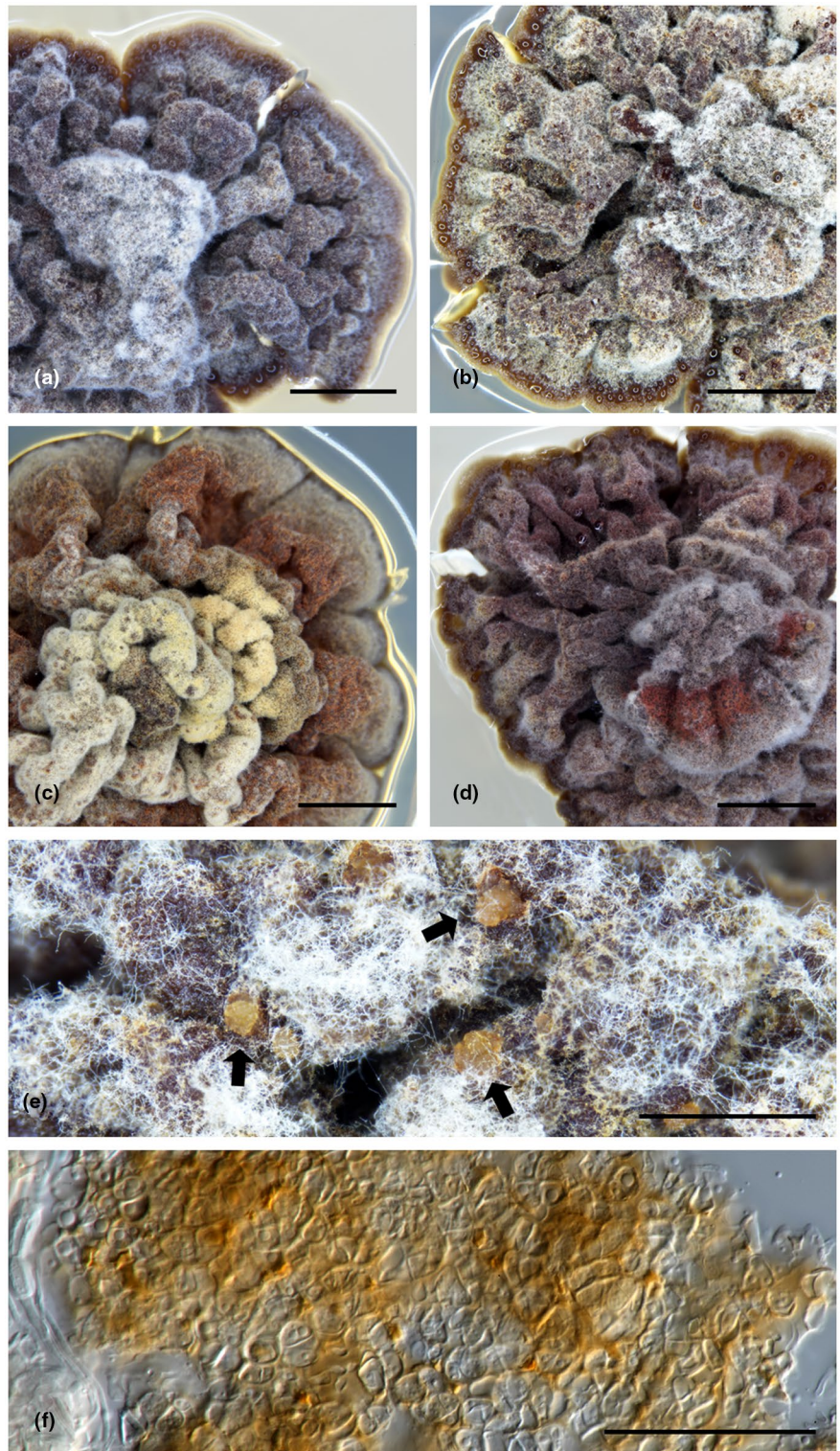
holotype, ex-holotype CMW 56134 = CBS 147439; PREM 63210, culture CMW 56137 = CBS 147440; Apr 2018, M.J. Wingfield & N.Q. Pham, PREM 63208, culture CMW 56129 = CBS 147438.

Distribution: North Sumatra, Indonesia.

Host: *Eucalyptus grandis* and *Eucalyptus urophylla* hybrids (*Eu. grandis* × *Eu. urophylla*).

Notes: In cross section, fungal hyphae and mycelial masses were observed in sections through necrotic lesions (scab) and not

FIGURE 5 Colony morphology of *Elsinoe necatrix* (CMW 56134 = CBS 147439 ex-holotype). (a–d) Upper view of colony on potato dextrose agar at 30 days at 25 °C in the dark (a–c) and under 12 hr dark/12 hr UV light cycle (d). (e) Close-up view of colony showing ball-like structure (arrows). (f) Squashed ball-like structure consisting of pseudoparenchymatous cells. Scale bars: a–d = 2.5 mm; e = 1 mm; f = 50 μ m



observed in healthy tissue. The histology of infected leaf lesions was typical of a scab disease (Figure 2).

3.5 | Pathogenicity tests

All three isolates of *El. necatrix* tested for pathogenicity on detached *Eu. grandis* branchlets produced necrotic spots similar to those found

under field conditions, 5–6 days postinoculation (Figure 6b). These infections were consistently absent from the negative controls (Figure 6a,b). The necrotic spots were abundant on the leaf laminae, which dried up and turned dark brown at their centres, where the margins were slightly raised, scab-like, and tan in colour after 14 days (Figure 6b). *El. necatrix* was consistently reisolated from the necrotic spots on the inoculated leaves and isolates were morphologically identical to those used in the pathogenicity test. The

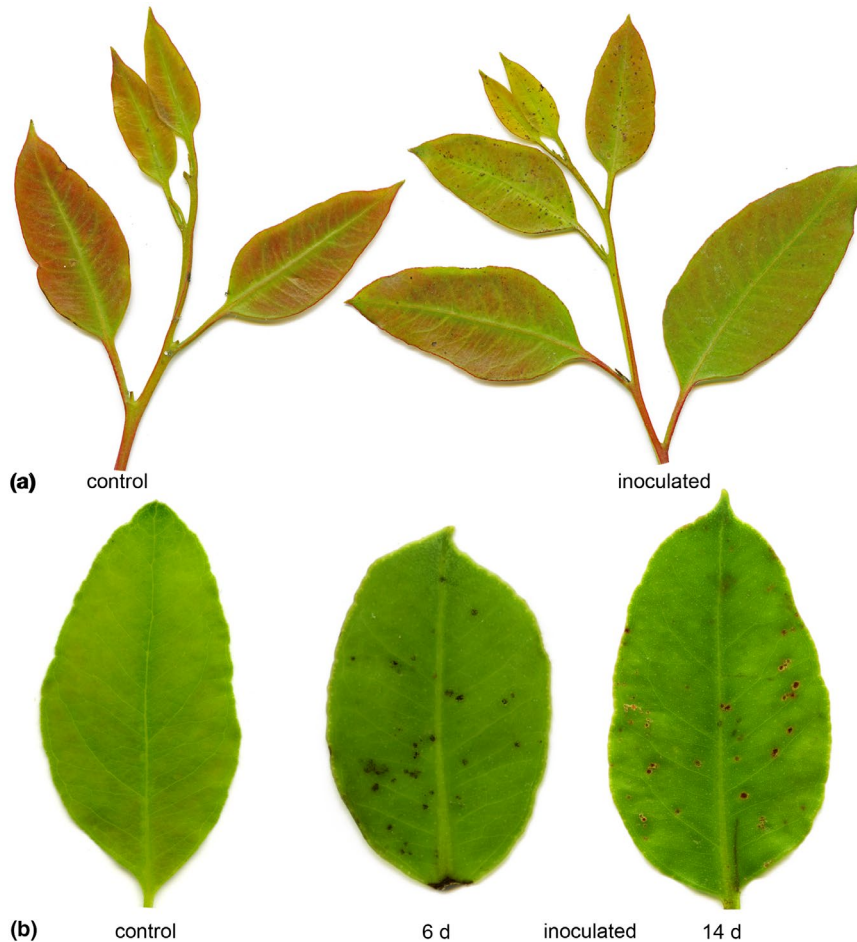


FIGURE 6 Results of inoculations with *Elsinoe necatrix* on detached *Eucalyptus grandis* branchlets. (a) Black necrotic spots on young leaves obvious after 10 days (right) and control free of symptoms (left). (b) The development of scab symptoms on young leaves, after 6 (middle) and 14 (right) days, compared to the control (left)

identity of these isolates was confirmed using DNA sequence data for the ITS region.

Scanning electron micrographs of *El. necatrix* infection on the adaxial surfaces of inoculated *Eu. grandis* leaves after 14 days showed that necrotic spots were slightly raised at their centres, with margins defined by deteriorated cuticle tissue (Figure 7a). Hyphae, conidiogenous cells, and conidia were obvious at the centres of all the necrotic spots (Figure 7b,c) and these were similar to those seen in micrographs from naturally infected tissues. Conidia observed on the surfaces of the necrotic spots were usually seen with emerging germ tubes (Figure 7d).

4 | DISCUSSION

The results of this study provide unequivocal evidence that an undescribed species of *Elsinoe* is the causal agent of a serious leaf and shoot disease affecting plantations of *Eucalyptus* in North Sumatra. This emerged from isolations made from lesions on leaves with symptoms, the identification of isolates based on DNA sequence analyses for four gene regions, and successful pathogenicity tests resulting in symptoms identical to those found under natural conditions. The causal agent of the disease was described as *El. necatrix*, a species name reflecting the severe impact that the disease has on

Eucalyptus trees. The most obvious and consistent symptom of the disease are the black scab-like lesions that develop on young leaves and shoots. Similar scab-like lesions are known for other *Elsinoe* pathogens and most notably citrus scab caused by *Elsinoe fawcettii* (Chung, 2011; Hyun et al., 2007). Consequently, we have chosen the name “Eucalyptus scab” for the disease and include “shoot malformation” referring to the secondary symptoms that consistently emerge on affected trees.

Phylogenetic inference based on DNA sequence comparisons has significantly improved the capacity to identify species and to elucidate the relationship between *Elsinoe* spp. and their host plants (Fan et al., 2017). In this study, phylogenetic analyses of ITS, LSU, *RPB2*, and *TEF1* individually, as well as the combination of these four gene regions, consistently revealed that isolates of *El. necatrix* represent a distinct clade. This was clearly separated from other previously described species in *Elsinoe* and supported by robust bootstrap and posterior probability values.

All previously reported species of *Elsinoe* on *Eucalyptus* have been described from Australia (Crous et al., 2016, 2019; Fan et al., 2017; Marin-Felix et al., 2019), where more than 700 species of *Eucalyptus* are endemic. As is true for many endemic fungi in their native environment, these fungi were not of any great concern regarding forest management, because they caused minor spots primarily on eucalypts in native habitats where their impact was

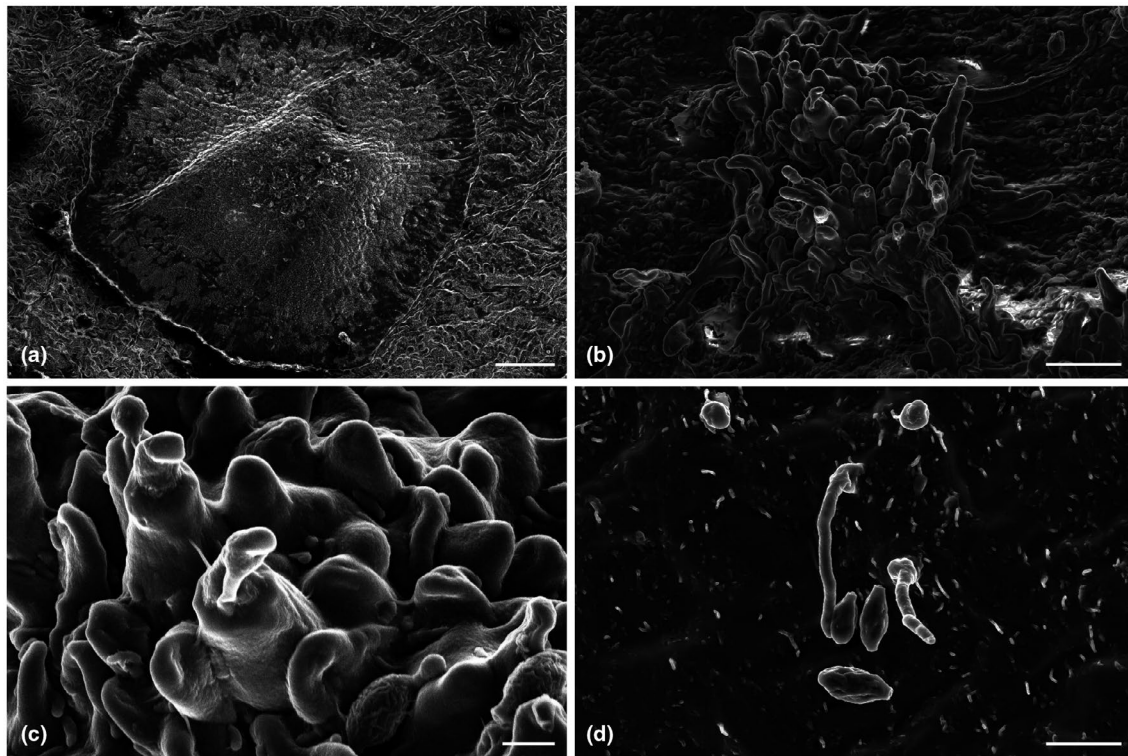


FIGURE 7 Scanning electron micrographs of *Elsinoe necatrix* infection on *Eucalyptus grandis* leaves 14 days after inoculation. (a) Necrotic spot with margin defined by deteriorated cuticle. (b,c) Hyphal system and conidiogenous cells in the middle of the necrotic spot. (d) Conidia observed on the surface of the necrotic spot. Scale bars: a = 100 μm , b = 10 μm , c, d = 5 μm

regarded as inconsequential (Crous et al., 2019). The discovery of *El. necatrix* causing a serious and important disease in the plantation forestry environment is the first time a species of *Elsinoe* has been found on nonnative *Eucalyptus* hosts.

The *Eucalyptus* disease discovered in this study first emerged in 2014 and it has taken approximately 6 years to identify the causal agent. The difficulty in identifying the cause of the disease can be attributed to a number of factors. These firstly include the fact that there is no known *Eucalyptus* disease with symptoms similar to those considered in this study. Secondly, the absence of any obvious microbial fruiting structures associated with infections led to a dependence on isolations from infected tissues without any clear link to any particular group of fungi. A third and important consideration was the fact that *Elsinoe* species are known to be notoriously difficult to isolate and have commonly been overlooked in early studies of diseases that they cause (Fan et al., 2017).

The discovery of *El. necatrix* exemplifies various challenges of working with this specific group of microfungi under laboratory conditions. Firstly, the development of a sexual morph is uncommon in nature, leading to difficulties in isolating and characterizing the fungi when no sporulation is obvious on the field specimens (Fan et al., 2017). The isolation process can also be challenging because *Elsinoe* spp. are easily outcompeted by other fast-growing opportunistic endophytic fungi or secondary contaminants. Furthermore, isolates of *Elsinoe* spp. are known to become sterile in culture, complicating the identification process (Fan et al., 2017). Although *El. necatrix*

could be seen sporulating on lesions emerging from natural infection using SEM, cultures of the fungus failed to produce spores in vitro. Nonetheless, we were able to reproduce the disease symptoms using mycelial fragments, and sporulation on the resulting lesions could be seen using SEM.

The origin of *El. necatrix* remains unknown, but this is an intriguing question that has significant relevance in terms of *Eucalyptus* plantation development globally. The pathogen might have been accidentally introduced into North Sumatra where it has encountered susceptible host trees and an environment conducive to infection. Such an introduction could have come from the area of origin of *Eucalyptus* including mainly Australia and nearby Indonesian islands (Thornhill et al., 2019). Alternatively, the pathogen could have emerged from native Myrtaceae that are common in Sumatra in close proximity to the plantation areas where the disease occurs. This would be similar to the situation with various other *Eucalyptus* pathogens such as species of *Chrysosporthe* (Gryzenhout et al., 2004; Nakabonge et al., 2006) and the myrtle rust pathogen *A. psidii* in South America (Glen et al., 2007).

Most species of *Elsinoe* are known to be host specific. Only four of the 82 accepted species occur on more than one host, and the remaining species are limited to a single host genus or species (Crous et al., 2019; Fan et al., 2017; Marin-Felix et al., 2019). Considering the narrow host range of species in this genus, it is less likely that *El. necatrix* underwent a host shift from an endemic plant to the exotic *Eucalyptus* plantations in Indonesia. Given the fact that *Eucalyptus*

plantations have been established in close proximity to endemic vegetation in the region of North Sumatra since 1987 (Pramono & Pudjiharta, 1996), the outbreak of *Eucalyptus* scab and shoot malformation only recently suggests a case of an introduced pathogen or a recent adaptation. The introduced hypothesis seems more feasible to us, considering all the information about the emergence and distribution of related species.

Field observations have shown clear evidence of significant differences in the susceptibility of different *Eucalyptus* hybrid clones to infection by *El. necatrix*. This suggests a high level of host specificity for the pathogen and it provides opportunities to avoid the problem in the future. This is similar to the situation with various other *Eucalyptus* disease problems that have been resolved through active breeding and selection for disease tolerance (van Heerden et al., 2005; Wingfield, 2003).

A number of diseases caused by fungal pathogens have seriously damaged plantations of *Eucalyptus* where these trees have been used as nonnative planting stock for commercial forestry (Burgess & Wingfield, 2017; Wingfield et al., 2015). Some of the more important of those affecting foliage and shoots include species of *Teratosphaeria*, such as *T. destructans* (Greyling et al., 2016; Old et al., 2003; Wingfield et al., 1996) and *T. nubilosa* (Andjic et al., 2019; Hunter et al., 2011; Pérez et al., 2009), and *A. psidii* (Carnegie et al., 2016; Coutinho et al., 1998; Glen et al., 2007). Of these, *Eucalyptus* scab and shoot malformation described in this study appears to be amongst the more destructive diseases. Consequently, *El. necatrix* requires further study in order to better understand its biology and the threat that it could pose to *Eucalyptus* plantations elsewhere in the world.






ACKNOWLEDGEMENTS

This study was initiated through the bilateral agreement between the Forestry and Agricultural Biotechnology Institute (FABI) and the April Group, RGE, Indonesia. The authors thank members of the April Group and Toba Pulp Lestari, RGE, Indonesia, particularly Paul Clegg, Santha Kumar, and Omar Syaref Purba for technical assistance in the field and technical advice.

DATA AVAILABILITY STATEMENT

The data that support the findings of this study are available from the corresponding author upon reasonable request.

ORCID

Nam Q. Pham  <https://orcid.org/0000-0002-4938-9067>
 Seonju Marincowitz  <https://orcid.org/0000-0002-4726-1211>
 Myriam Solís  <https://orcid.org/0000-0001-6468-135X>
 Tuan A. Duong  <https://orcid.org/0000-0001-5110-1854>
 Brenda D. Wingfield  <https://orcid.org/0000-0002-6189-1519>
 Irene Barnes  <https://orcid.org/0000-0002-4349-3402>
 Bernard Slippers  <https://orcid.org/0000-0003-1491-3858>
 Jupiter I. Muro Abad  <https://orcid.org/0000-0003-3006-0955>
 Alvaro Durán  <https://orcid.org/0000-0002-3035-9087>
 Michael J. Wingfield  <https://orcid.org/0000-0001-9346-2009>

REFERENCES

- Alfenas, R.F., Lombard, L., Pereira, O.L., Alfenas, A.C. & Crous, P.W. (2015) Diversity and potential impact of *Calonectria* species in *Eucalyptus* plantations in Brazil. *Studies in Mycology*, 80, 89–130.
- Andjic, V., Carnegie, A.J., Pegg, G.S., Hardy, G.E., St, J., Maxwell, A. et al. (2019) 23 years of research on *Teratosphaeria* leaf blight of *Eucalyptus*. *Forest Ecology and Management*, 443, 19–27.
- Burgess, T.I. & Wingfield, M.J. (2017) Pathogens on the move: a 100-year global experiment with planted eucalypts. *BioScience*, 67, 14–25.
- Carnegie, A.J., Kathuria, A., Pegg, G.S., Entwistle, P., Nagel, M. & Giblin, F.R. (2016) Impact of the invasive rust *Puccinia psidii* (myrtle rust) on native Myrtaceae in natural ecosystems in Australia. *Biological Invasions*, 18, 127–144.
- Chung, K.R. (2011) *Elsinoë fawcettii* and *Elsinoë australis*: the fungal pathogens causing citrus scab. *Molecular Plant Pathology*, 12, 123–135.
- Cossalter, C. & Pye-Smith, C. (2003) *Fast-Wood Forestry: Myths & Realities*. Jakarta, Indonesia: Center for International Forestry Research.
- Coutinho, T.A., Wingfield, M.J., Alfenas, A.C. & Crous, P.W. (1998) *Eucalyptus* rust: A disease with the potential for serious international implications. *Plant Disease*, 82, 819–825.
- Crous, P.W. (2002) *Taxonomy and Pathology of Cyliandrocladium (Calonectria) and Allied Genera*. St Paul, MN, USA: APS Press.
- Crous, P.W., Wingfield, M.J., Burgess, T.I., Hardy, G.E., St. J., Crane, C. et al. (2016) Fungal Planet description sheets: 469–557. *Persoonia*, 37, 218–403.
- Crous, P.W., Wingfield, M.J., Cheewangkoon, R., Carnegie, A.J., Burgess, T.I., Summerell, B.A. et al. (2019) Foliar pathogens of eucalypts. *Studies in Mycology*, 94, 125–298.
- Fan, X.L., Barreto, R.W., Groenewald, J.Z., Bezerra, J.D.P., Pereira, O.L., Cheewangkoon, R. et al. (2017) Phylogeny and taxonomy of the scab and spot anthracnose fungus *Elsinoë* (Myriangiales, Dothideomycetes). *Studies in Mycology*, 87, 1–41.
- Ghelardini, L., Pepori, A.L., Luchi, N., Capretti, P. & Santini, A. (2016) Drivers of emerging fungal diseases of forest trees. *Forest Ecology and Management*, 381, 235–246.
- Glen, M., Alfenas, A.C., Zauza, E.A.V., Wingfield, M.J. & Mohammed, C. (2007) *Puccinia psidii*: a threat to the Australian environment and economy – a review. *Australasian Plant Pathology*, 36, 1–16.
- Greyling, I., Wingfield, M.J., Coetzee, M.P.A., Marincowitz, S. & Roux, J. (2016) The *Eucalyptus* shoot and leaf pathogen *Teratosphaeria destructans* recorded in South Africa. *Southern Forests*, 78, 123–129.
- Gryzenhout, M., Myburg, H., Van der Merwe, N.A., Wingfield, B.D. & Wingfield, M.J. (2004) *Chrysosporthe*, a new genus to accommodate *Cryphonectria cubensis*. *Studies in Mycology*, 50, 119–142.
- van Heerden, S.W., Amerson, H.V., Preisig, O., Wingfield, B.D. & Wingfield, M.J. (2005) Relative pathogenicity of *Cryphonectria cubensis* on *Eucalyptus* clones differing in their resistance to *C. cubensis*. *Plant Disease*, 89, 659–662.
- Hunter, G.C., Crous, P.W., Carnegie, A.J., Burgess, T.I. & Wingfield, M.J. (2011) *Mycosphaerella* and *Teratosphaeria* diseases of *Eucalyptus*; easily confused and with serious consequences. *Fungal Diversity*, 50, 145–166.
- Hurley, B.P., Garnas, J., Wingfield, M.J., Branco, M., Richardson, D.M. & Slippers, B. (2016) Increasing numbers and intercontinental spread of invasive insects on eucalypts. *Biological Invasions*, 18, 921–933.
- Hyun, J.W., Timmer, L., Lee, S.C., Yun, S.H., Ko, S.W. & Kim, K.S. (2007) Pathological characterization and molecular analysis of *Elsinoë* isolates causing scab diseases of citrus in Jeju Island in Korea. *Plant Disease*, 85, 1013–1017.
- Katoh, K. & Standley, D.M. (2013) MAFFT multiple sequence alignment software version 7: improvements in performance and usability. *Molecular Biology and Evolution*, 30, 772–780.
- Keane, P.J., Kile, G.A., Podger, F.D. & Brown, B.N. (2000) *Diseases and Pathogens of Eucalypts*. Collingwood, Australia: CSIRO Publishing.
- Kearse, M., Moir, R., Wilson, A., Stones-Havas, S., Cheung, M., Sturrock, S. et al. (2012) Geneious Basic: an integrated and extendable desktop

- software platform for the organization and analysis of sequence data. *Bioinformatics*, 28, 1647–1649.
- Kumar, S., Stecher, G. & Tamura, K. (2016) MEGA7: molecular evolutionary genetics analysis version 7.0 for bigger datasets. *Molecular Biology and Evolution*, 33, 1870–1874.
- Liu, Y.J., Whelen, S. & Hall, B.D. (1999) Phylogenetic relationships among ascomycetes: evidence from an RNA polymerase II subunit. *Molecular Biology and Evolution*, 16, 1799–1808.
- Lombard, L., Chen, S.F., Mou, X., Zhou, X.D., Crous, P.W. & Wingfield, M.J. (2015) New species, hyper-diversity and potential importance of *Calonectria* spp. from *Eucalyptus* in South China. *Studies in Mycology*, 80, 151–188.
- Marin-Felix, Y., Hernández-Restrepo, M., Iturrieta-González, I., García, D., Gené, J., Groenewald, J.Z. et al. (2019) Genera of phytopathogenic fungi: GOPHY 3. *Studies in Mycology*, 94, 1–124.
- Nakabonge, G., Roux, J., Gryzenhout, M. & Wingfield, M.J. (2006) Distribution of *Chrysosporthe* canker pathogens on *Eucalyptus* and *Syzygium* spp. in eastern and southern Africa. *Plant Disease*, 90, 734–740.
- Old, K.M., Wingfield, M.J. & Yuan, Z.Q. (2003) *A Manual of Disease of Eucalypts in South-East Asia*. Jakarta, Indonesia: Center for International Forestry Research.
- Paine, T.D., Steinbauer, M.J. & Lawson, S.A. (2011) Native and exotic pests of *Eucalyptus*: a worldwide perspective. *Annual Review of Entomology*, 56, 181–201.
- Payn, T., Carnus, J.M., Freer-Smith, P., Kimberley, M., Kollert, W., Liu, S. et al. (2015) Changes in planted forests and future global implications. *Forest Ecology and Management*, 352, 57–67.
- Pérez, G., Hunter, G.C., Slippers, B., Pérez, C., Wingfield, B.D. & Wingfield, M.J. (2009) *Teratosphaeria* (*Mycosphaerella*) *nubilosa*, the causal agent of *Mycosphaerella* leaf disease (MLD), recently introduced into Uruguay. *European Journal of Plant Pathology*, 125, 109–118.
- Pham, N.Q., Barnes, I., Chen, S., Liu, F., Dang, Q.N., Pham, T.Q. et al. (2019) Ten new species of *Calonectria* from Indonesia and Vietnam. *Mycologia*, 111, 78–102.
- Posada, D. (2008) jModelTest: phylogenetic model averaging. *Molecular Biology and Evolution*, 25, 1253–1256.
- Pramono, I.B. & Pudjiharta, A. (1996) Research experiences on *Eucalyptus* in Indonesia. In: Kashio, M. and White, K. (Eds.) *Reports Submitted to the Regional Expert Consultation on Eucalyptus*. Bangkok: RAP Publication (FAO), pp. 75–83.
- Rayner, R.W. (1970) *A Mycological Colour Chart*. Kew, UK: Commonwealth Mycological Institute.
- Rehner, S.A. & Samuels, G.J. (1994) Taxonomy and phylogeny of *Gliocladium* analysed from nuclear large subunit ribosomal DNA sequences. *Mycological Research*, 98, 625–634.
- Ronquist, F., Teslenko, M., van der Mark, P., Ayres, D.L., Darling, A., Höhna, S. et al. (2012) MrBayes 3.2: efficient Bayesian phylogenetic inference and model choice across a large model space. *Systematic Biology*, 61, 539–542.
- Stamatakis, A. (2014) RAxML version 8: a tool for phylogenetic analysis and post-analysis of large phylogenies. *Bioinformatics*, 30, 1312–1313.
- Sung, G.H., Sung, J.M., Hywel-Jones, N.L. & Spatafora, J.W. (2007) A multi-gene phylogeny of Clavicipitaceae (Ascomycota Fungi): identification of localized incongruence using a combinational bootstrap approach. *Molecular Phylogenetics and Evolution*, 44, 1204–1223.
- Thornhill, A.H., Crisp, M.D., Külheim, C., Lam, K.E., Nelson, L.A., Yeates, D.K. et al. (2019) A dated molecular perspective of eucalypt taxonomy, evolution and diversification. *Australian Systematic Botany*, 32, 29–48.
- Vilgalys, R. & Hester, M. (1990) Rapid genetic identification and mapping of enzymatically amplified ribosomal DNA from several *Cryptococcus* species. *Journal of Bacteriology*, 172, 4238–4246.
- White, T.J., Bruns, T., Lee, S. & Taylor, J.W. (1990) Amplification and direct sequencing of fungal ribosomal RNA genes for phylogenetics. In: Innis, M.A., Gelfand, D.H., Sninsky, J.J. and White, T.J. (Eds.) *PCR Protocols: A Guide to Methods and Applications*. San Diego, CA, USA: Academic Press, pp. 315–322.
- Wingfield, M.J. (2003) Increasing threat of diseases to exotic plantation forests in the Southern Hemisphere: lessons from *Cryphonectria* canker. *Australasian Plant Pathology*, 32, 133–139.
- Wingfield, M.J., Brockerhoff, E.G., Wingfield, B.D. & Slippers, B. (2015) Planted forest health: The need for a global strategy. *Science*, 349, 832–836.
- Wingfield, M.J., Crous, P.W. & Boden, D. (1996) *Kirramyces destructans* sp. nov., a serious leaf pathogen of *Eucalyptus* in Indonesia. *South African Journal of Botany*, 62, 325–327.
- Wingfield, M.J., Slippers, B., Hurley, B.P., Coutinho, T.A., Wingfield, B.D. & Roux, J. (2008) Eucalypt pests and diseases: growing threats to plantation productivity. *Southern Forests*, 70, 139–144.
- Wingfield, M.J., Slippers, B. & Wingfield, B.D. (2010) Novel associations between pathogens, insects, and tree species threaten world forests. *New Zealand Journal of Forestry Science*, 40, S95–S103.

SUPPORTING INFORMATION

Additional supporting information may be found online in the Supporting Information section.

How to cite this article: Pham NQ, Marincowitz S, Solís M, et al. Eucalyptus scab and shoot malformation: A new and serious foliar disease of *Eucalyptus* caused by *Elsinoe necatrix* sp. nov. *Plant Pathol.* 2021;00:1–13. <https://doi.org/10.1111/ppa.13348>